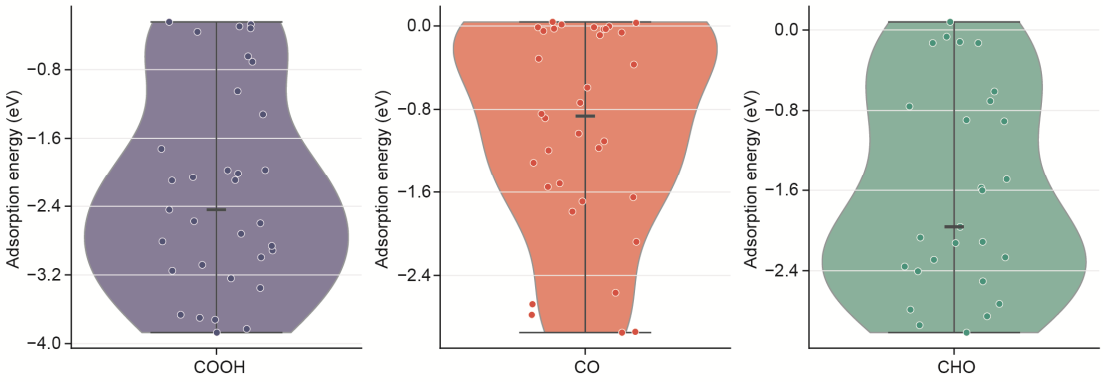


Figure S1. Adsorption-energy distributions for the three C1 probes. Violin distributions and individual metal values for COOH, CO, and CHO adsorption. Horizontal markers show central tendencies. The panels emphasize broad coverage and adsorbate-dependent ranges without implying identical distribution shapes.

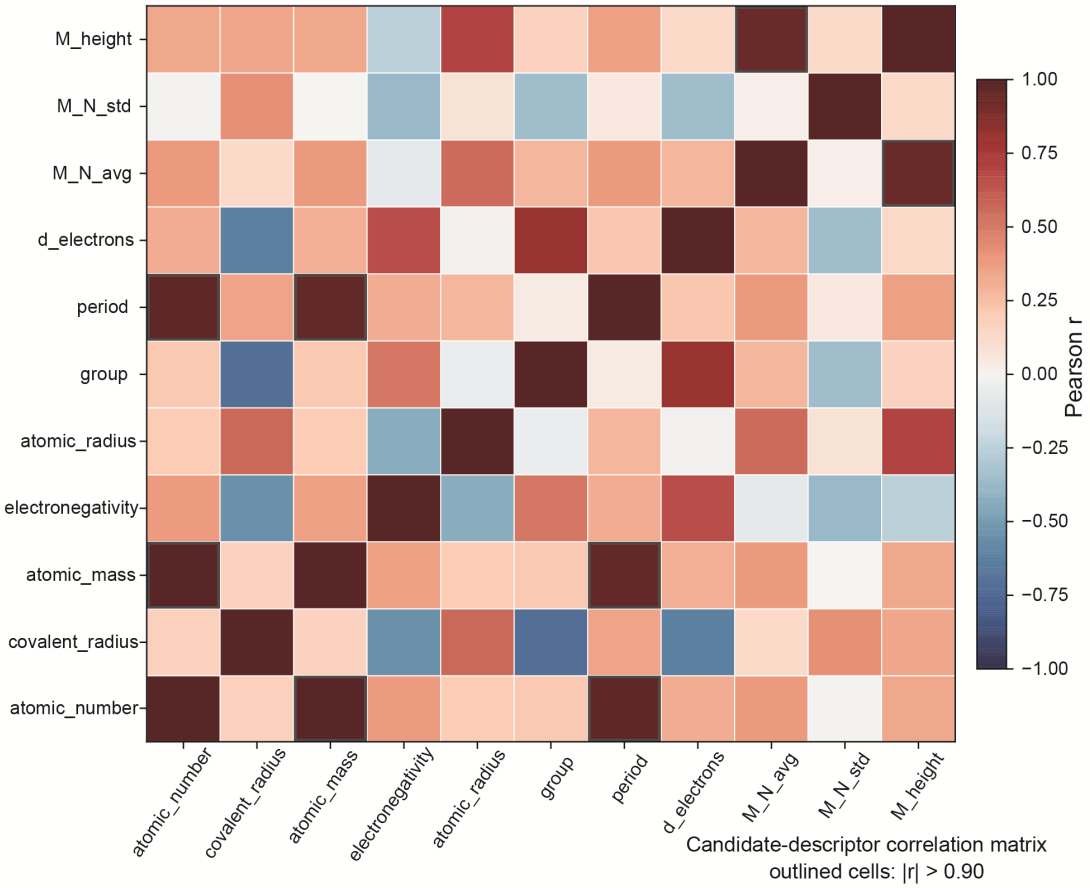


Figure S2. Correlation matrix for the 11 candidate descriptors. Pairwise Pearson correlations among elemental, electronic, and local structural descriptors. Outlined cells mark $|r| > 0.900$, demonstrating substantial redundancy that motivates joint interpretation of permutation importance, direct DFT correlations, and out-of-fold SHAP values.

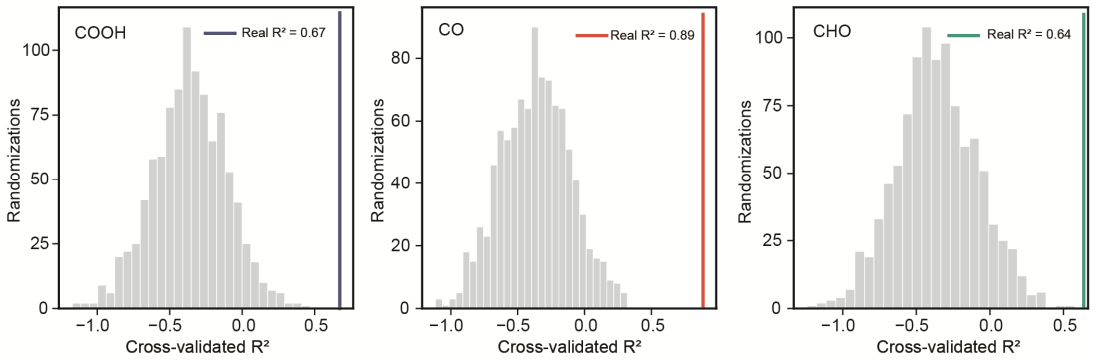


Figure S3. Target-randomization tests for adsorption-energy models. Cross-validated R^2 distributions from 1,000 independently shuffled targets for each adsorbate. Vertical colored lines show performance for the unshuffled targets. The separation corresponds to an empirical significance of approximately p = 0.001 and indicates that the predictive signal is unlikely to be due to random association.

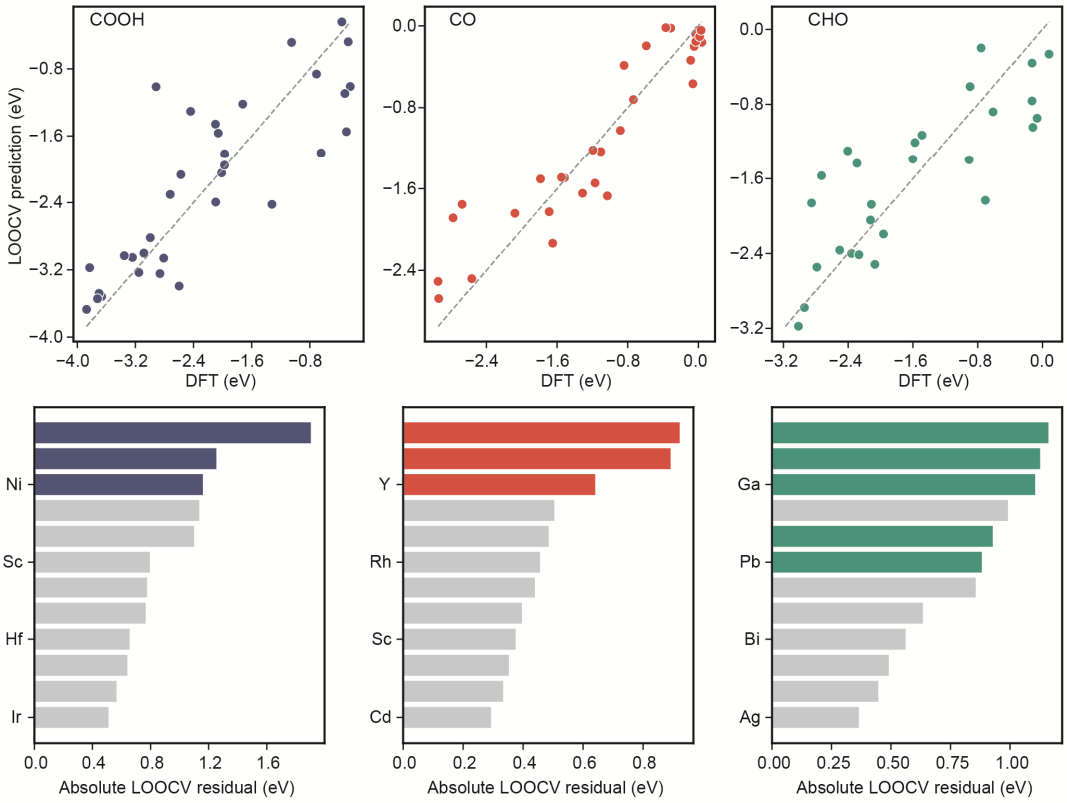


Figure S4. Leave-one-out prediction and residual diagnostics. Top panels compare leave-one-out predictions with DFT energies for COOH, CO, and CHO; dashed lines denote parity. Bottom panels rank absolute sample-level residuals and highlight selected high-residual metals. These results provide a sample-level robustness check; headline model metrics are the nested out-of-fold values in Figure 2.

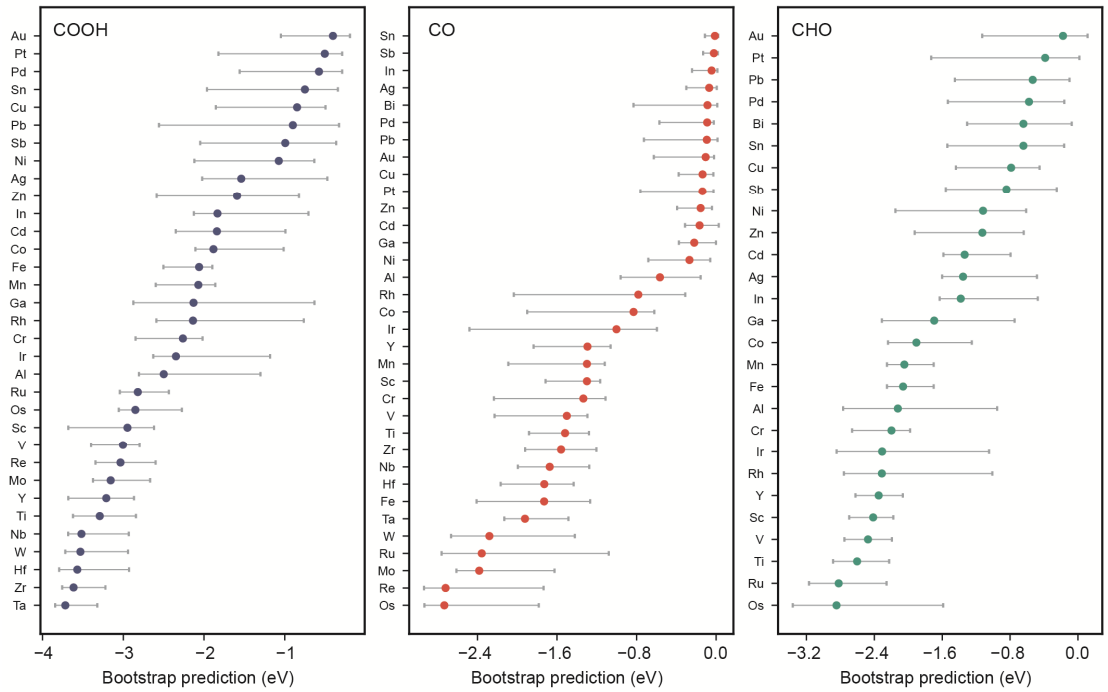


Figure S5. Bootstrap prediction stability. Central predictions and horizontal variability intervals from 1,000 bootstrap resamples for COOH, CO, and CHO, ordered by central predicted energy. Interval widths vary among metals and quantify sensitivity to resampling; they are not a catalyst-ranking metric.

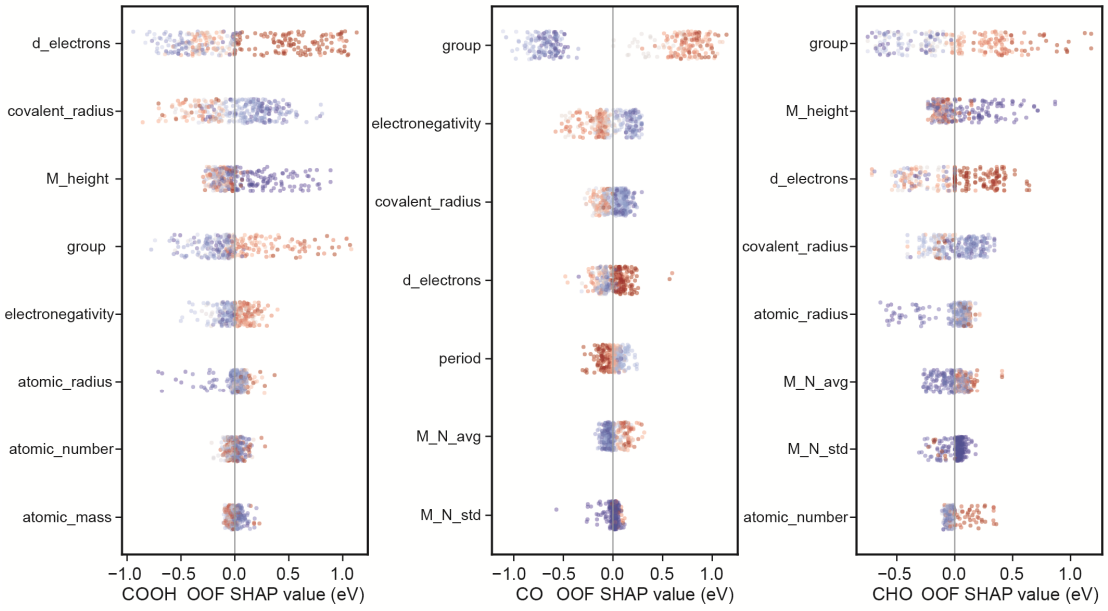


Figure S6. Out-of-fold SHAP summaries for the selected models. Each point shows an out-of-fold feature contribution for COOH, CO, or CHO. Positive SHAP values shift predicted adsorption energy upward, and negative values shift it downward. Color represents low-to-high feature value. The summaries support directional descriptor trends but do not establish causality.

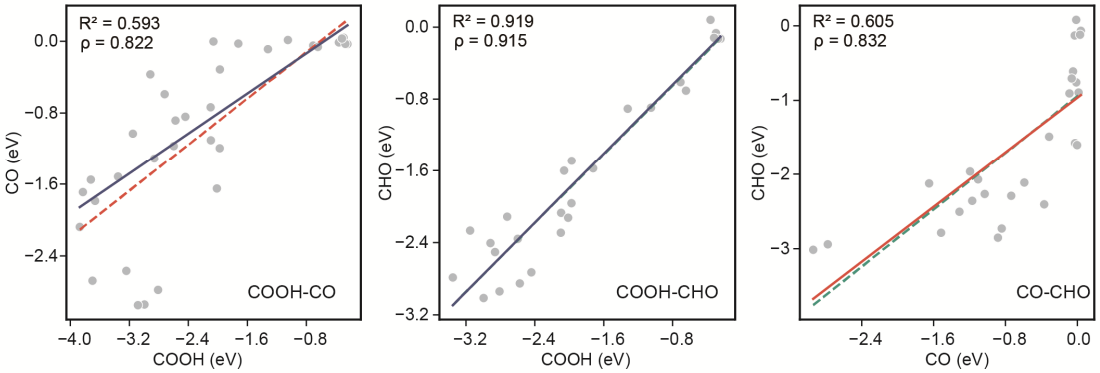


Figure S7. Pairwise scaling relationships among COOH, CO, and CHO adsorption energies. Ordinary least-squares fits are dashed, and Huber fits are solid. COOH–CO gives n = 33, slope = 0.647, R^2 = 0.593, and Spearman ρ = 0.822; COOH–CHO gives n = 26, slope = 0.956, R^2 = 0.919, and Spearman ρ = 0.915; CO–CHO gives n = 27, slope = 0.956, R^2 = 0.605, and Spearman ρ = 0.832. COOH–CHO is the strongest linear relationship, while the CO-containing pairs exhibit larger residual variation.